ACS OMEGA

Open Access

http://pubs.acs.org/journal/acsodf

Article

Investigation of Filtration and Shale Inhibition Characteristics of Chitosan-*N*-(2-hydroxyl)-propyl trimethylammonium Chloride as Drilling Fluid Additives

Amolina Doley, Vikas Mahto, Vinay Kumar Rajak,* Raj Kiran, and Rajeev Upadhyay

Cite This: *ACS Omega* 2024, 9, 21365−21377

Read Online

ACCESS | Metrics & More | Article Recommendations | Supporting Information

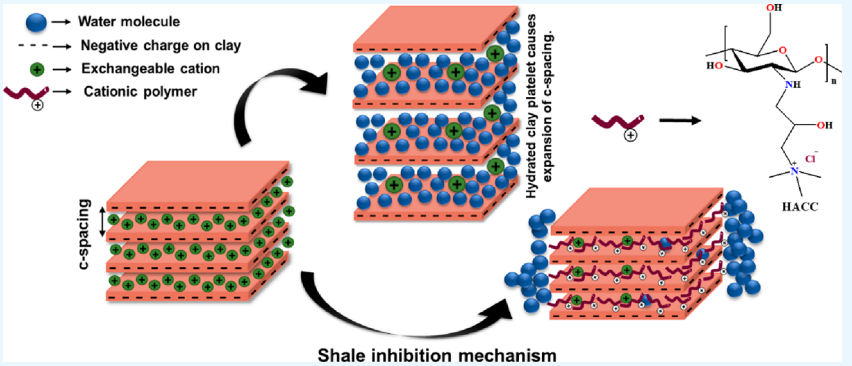

ABSTRACT: Hydrated shale formations often lead to severe drilling problems and may lead to wellbore instability. These instabilities can result in issues such as bit balling, borehole collapse, formation damage, stuck pipe, and low drilling rates. Keeping these fundamental issues with drilling in shale formation in mind, this study is aimed at designing a water-based drilling fluid system for effective shale inhibition, ensuring enhanced wellbore stability and drilling efficiency. The designed mud system comprises a typical base fluid along with newly synthesized chitosan derivative chitosan-*N*-(2-hydroxyl)-propyl trimethylammonium chloride (HACC) as an additive. This additive was found to be soluble in water and conducive for shale inhibition. The derived product was characterized by field emission scanning electron microscopy, thermogravimetric analysis, and Fourier-transform infrared spectroscopy (FTIR). Various drilling fluid tests, including filtration and rheological experiments, were conducted to evaluate its proficiency as a drilling mud additive. The results showed improvement in rheological and filtration properties after hot rolling at 100 °C in comparison to a conventional shale inhibitor, polyethylenimine. As we increase the concentration of synthesized chitosan derivative from 0.3 to 1.5 w/v%, the filtration loss is reduced from 40% to 65% as compared to the base fluids. Shale recovery tests were also conducted using shale samples from an Indian field to assess its viability for field application. The addition of 0.3 to 1.5 w/v% chitosan derivative resulted in high shale recovery above 88% to 96% at 100 °C compared to polyethylenimine, which showed a change in recovery from 62% to 73%. HACC intercalates into clay platelets, reducing the interlayer spacing between particles and preventing clay from hydrating and swelling. This mechanism of inhibition is evaluated by X-ray diffraction, FTIR, and zeta potential analysis. This bolsters the hypothesis of using the synthesized chitosan derivative as a shale inhibitor.

1. INTRODUCTION

In this energy-intensive era, shale is considered to be one of the most vital unconventional resources in the world. The presence of mud, clay, and silt in shale formations makes it a complex entity that requires extra care during resource exploitations.[1,2] The clay minerals found in shale are crystalline and flaky and structured in the layered form.[3] Chemically, they are mica crystals with sheets that are either tetrahedral or octahedral. In the tetrahedral sheet, four oxygen atoms are bound to a core silicon atom as opposed to the octahedral sheet, which contains a central metal atom (often aluminum) surrounded by six oxygen atoms. These sheets are joined through the weak van der Waals force via the oxygen atom forming a cleavage plane between the platelets.[4] Due to the presence of water, the water molecule gets trapped between these platelets and consequently causes swelling and dispersion.[5] The presence of clay particles makes the shale formations vulnerable to water absorption resulting in the oil and gas operational complexity.[6]

Received: February 20, 2024
Revised: April 18, 2024
Accepted: April 19, 2024
Published: May 1, 2024

Oil production from these shale formations can be a formidable avenue to satisfy the energy demand. However, the drilling operations in these shale formations are often marred with various issues including fluid loss, differential sticking, and wellbore instability.[7,8] The most problematic and recurrent issue that might arise during a drilling operation is wellbore instability. To reduce the nonproductive time and ensure optimized operation throughout the drilling process, the borehole quality should be maintained properly. Low drilling rate, formation damage, stuck pipe, borehole collapse, and shale hydration are some of the key wellbore instability characteristics.[9] These problems occur frequently, have caused a huge economic loss, and have restricted the development of shale gas. The success of drilling is largely determined by the performance of the drilling fluid.[10,11] Drilling fluid helps clean up cuttings, balance formation pressure, stabilize the borehole wall, and cool and lubricate drilling equipment during the drilling operation.[12,13] Although oil-based drilling fluids inhibit shale hydration, they are hazardous to the environment, especially when applied to aquatic ecosystems.[14] Therefore, water-based drilling fluid is the most widely used system because of its low toxicity and low cost.

Besides the ability to efficiently reduce shale hydration, compatibility with other additives is critical for an effective high-performance drilling fluid.[15] The ideal shale inhibitor will be efficient, thermally stable, compatible, and biodegradable. There are various inhibitors, including amines, acrylamides, imines, glycerol, glycols, silicates, and biomolecules, generally used in shale operations. Potassium salts are widely used and are one of the earliest shale inhibitors used in the industry.[16] The swelling of the clay minerals is restricted due to ion exchange between the inhibitor and the existing clay minerals. The potassium salts and polymers were combined to reduce the salt concentrations in water-based mud and consequently exhibited better inhibition properties than pure potassium chloride (KCl).[17,18] Besides the potassium salts, partially hydrolyzed polyacrylamide is also being used for shale inhibition purposes.[19] The other inhibitors such as salts,[20] polyglycerols,[21] polyglycols,[22] and silicates[23] exhibit certain limitations. These limitations include vulnerability with specific ions such as carbonate and phosphate, negative impact on rheological and filtration properties, reduced performance at high pH levels, limited mechanical stability, and environmental constraints.[24,25]

Amine-based inhibitors including quaternary, oligomeric, and polymeric quaternary amines are also used for constraining the clay swelling.[26] The amine-based cationic shale inhibitors can substitute for sodium ions in a clay lattice. Additionally, these inhibitors exhibit characteristics such as reduced toxicity, enhanced stability, efficient inhibition, and biodegradability, making them preferable candidates for shale drilling mud additive. Chitosan is another additive, derived from the partial deacetylation of chitin, a naturally occurring linear polysaccharide that constitutes a biocompatible, nontoxic cationic polymer.[27,28] Glucosamine and *N*-acetylglucosamine residues with a 1,4-β-linkage constitute chitosan, the second most abundant natural polymer next to cellulose.[29] On account of its excellent biocompatibility, biodegradability, nontoxicity, antimicrobial activity, and economic benefits, chitosan is considered a favorable material for future applications.[30] Despite these advantages, chitosan is not soluble in water, which limits its use in a variety of fields. Efforts are being made by researchers to overcome this limitation, by enhancing its solubility and, thereby, expanding its applications.[31]

Keeping the uniqueness of chitosan in mind, water-soluble chitosan-*N*-(2-hydroxyl)-propyl trimethylammonium chloride (HACC) was tested for its applicability as a shale inhibitor. First of all, it was synthesized and characterized using various techniques including thermogravimetric analysis (TGA), Fourier-transform infrared spectroscopy (FTIR), energy-dispersive X-ray (EDX), and field-emission scanning electron microscopy (FESEM). Due to its polyampholyte nature, this chitosan derivative tends to form polyelectrolyte complexes.[32] As a result, it is useful as an additive to water-based drilling mud, which was surveyed by using rheological and filtration tests. A mixture of synthesized quaternary amine, xanthan gum (XG), bentonite, and KCl was evaluated for shale inhibition. The shale recovery tests were conducted, and the results were compared with those of polyethylenimine (PEI) (a conventional shale inhibitor) to assess its suitability as an additive.

2. MATERIALS AND METHODS

2.1. Materials Used. The chitosan derivative was synthesized using various procured chemicals. These chemicals included (3-chloro-2-hydroxypropyl) trimethylammonium chloride, polyethylenimine, chitosan (CS), and sodium hydroxide (NaOH) (from Sigma-Aldrich, TCI Chemicals Pvt. Ltd., Sisco Research Laboratories Pvt. Ltd.). Other chemicals including XG, KCl, and industrial grade bentonite clay were obtained from Oil & Natural Gas Corporation Ltd. (ONGC), to prepare the drilling fluid. The shale cuttings were obtained from an Indian oil field located in the central India. The workflow of our detailed study is shown in Figure 1.

2.2. Synthesis of Chitosan-N-(2-hydroxyl)-propyl trimethylammonium Chloride (HACC). Figure 2 presents the chemical reaction involved in the synthesis of HACC. First, 100 mL of deionized water is taken in a 500 mL three-necked flask, and 8 g of chitosan along with 2 g of NaOH is added to it. The round-bottom flask was placed into an oil bath to heat it at an appropriate temperature for the reaction to begin. Twenty milliliters of (3-chloro-2-hydroxypropyl) trimethylammonium chloride solution is added to the mixture and stirred at a temperature of 70 °C for 24 h. The three-neck flask was used for nitrogen purging, using a condenser and placing a thermometer through each vent. The thermometer was attached to monitor the temperature. After 24 h, the solution was cooled down and acetone was added. The mixture was further put into centrifuge tubes to separate the solid and liquid parts. The solid product was washed 3 times to remove unreacted chemicals and impurities.[33−36]

2.3. Characterization of HACC. *2.3.1. FTIR Spectroscopy.* The PerkinElmer Spectrum Two FTIR instrument (USA) was used to obtain the peaks for the characterization of various functional groups. Potassium bromide-based pellets were prepared by applying 100 psi pressure in a hydraulic press for 60 s. The pellets consisted of a mixture containing 1 mg of the HACC sample and 100 mg of KBr. 100 scans were conducted to obtain the infrared spectrum of these pellets. The spectral noise was removed, and the data was analyzed for the presence of various functional groups. These functional groups can be used to confirm the formation of HACC.

2.3.2. TGA. TGA provides the weight change in the sample while it is heated at a consistent rate. This analysis can be used to establish the thermal stability of the sample and the percentage of volatile components in it. In this study, the

https://doi.org/10.1021/acsomega.4c01632
ACS Omega 2024, 9, 21365−21377

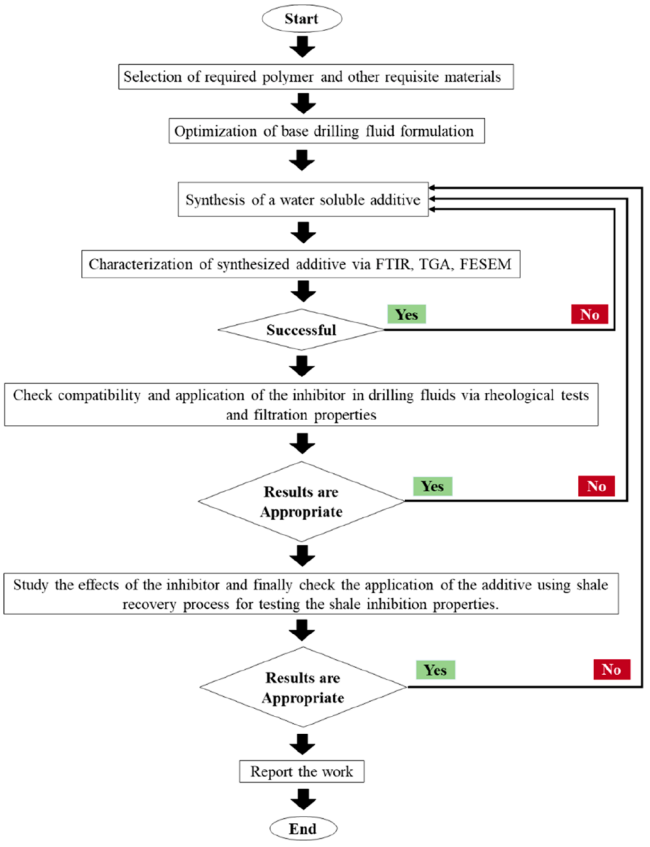

Figure 1. Overview of the study workflow.

thermal stability and derived thermogravimetric analysis (DTG) of the synthesized chitosan derivative (HACC) and chitosan were compared in a nitrogen atmosphere under a heating rate of 10 °C per minute from 35 to 800 °C.

2.3.3. FESEM and EDX. The surface morphology and elemental composition of chitosan and HACC were obtained by using FESEM and energy-dispersive X-ray spectroscopy. The test was conducted using the FESEM Supra 55 model Carl Zeiss (Germany) with an Air Lock chamber. The samples were coated with gold, and the FESEM images along with the elemental compositions of the samples were obtained.

2.4. Characterization of Shale Cuttings. The clay composition of shale samples was characterized using FESEM, EDX, X-ray diffraction (XRD), wavelength-dispersive X-ray fluorescence (XRF), and cation exchange capacity (CEC) as reported by Doley et al. (2023).[37] The CEC of used shale samples was found to be 15 mequiv/100 g. The EDX, XRF, and XRD results showed a significant amount of quartz and clay minerals, such as montmorillonite and kaolinite. The FESEM results showed the presence of a few undulations on the surface which can be attributed to the stacking of the sheets and crystalline arrangement.

2.5. Drilling Mud Formulation. By combining 3 w/v% bentonite and 5 w/v% KCl, a drilling mud formulation was prepared.[38] It was mixed constantly with the help of a mechanical stirrer for 30 min to form a homogeneous mixture, and the rheological parameters such as plastic viscosity (PV), yield point (YP), apparent viscosity (AV), initial gel strength (IG), and final gel strength (FG) of this formulation were measured, and the result is shown in Table 1. Following that, various concentrations of HACC were introduced into the bentonite dispersion to evaluate its effects on the various drilling fluid parameters in accordance with American Petroleum Institute (API) protocols, but the desired viscosity was not obtained for the different drilling fluid formulations (Table 2). Therefore, in order to enhance the properties of the drilling fluid formulation, different concentrations of XG were incorporated into the fluid formulation to obtain the desired properties. First of all, along with 3 w/v% bentonite and 5 w/v % KCl, 0.3 w/v% of XG was introduced into the formulation, which was termed Base mud 1. Similarly, introducing 0.4 w/v%

Table 1. Rheological Parameters of 3 w/v% Bentonite + 5 w/v% KCl

Properties	PV (cP)	YP (lb/100 ft^2)	AV (cP)	IG (lb/100 ft^2)	FG (lb/100 ft^2)
Observed values	1.5	1	2	2	2.5

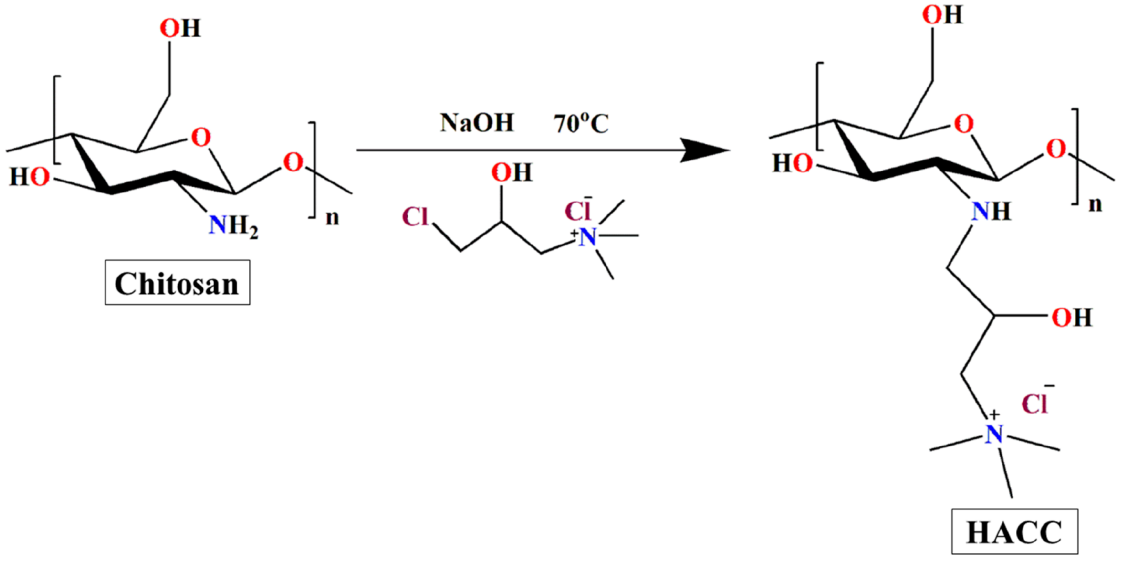

Figure 2. Schematic representation of the synthesis process of HACC.

https://doi.org/10.1021/acsomega.4c01632
ACS Omega 2024, 9, 21365−21377

Table 2. Effect of HACC on 3 w/v% Bentonite + 5 w/v% KCl

Properties	0.3 w/v%	0.6 w/v%	0.9 w/v%	1.2 w/v%	1.5 w/v%
PV (cP)	2	2.5	3.5	5	6
YP (lb/100 ft^2)	1	2	3	3	4
AV (cP)	2.5	3.5	5	6.5	8
IG (lb/100 ft^2)	2	2.5	3	4	4
FG (lb/100 ft^2)	3.5	4	6	6	6

and 0.5 w/v% of XG to the formulation was termed Base mud 2 and Base mud 3, respectively. Hence in this paper, we have evaluated 34 different formulations of water-based drilling mud, which is shown in Table 3.

Table 3. Different Formulations of Water-Based Drilling Mud

Sl. no	Formulation (w/v%)
1	Base mud = 3 w/v% bentonite + 5 w/v% KCl + XG (0.3, 0.4, or 0.5 w/v%)
2	Base mud 1 + HACC (0.3, 0.6, 0.9, 1.2, and 1.5) w/v%
3	Base mud 1 + PEI (0.3, 0.6, 0.9, 1.2, and 1.5) w/v%
4	Base mud 2 + HACC (0.3, 0.6, 0.9, 1.2, and 1.5) w/v%
5	Base mud 2 + PEI (0.3, 0.6, 0.9, 1.2, and 1.5) w/v%
6	Base mud 3 + HACC (0.3, 0.6, 0.9, 1.2, and 1.5) w/v%
7	Base mud 3 + PEI (0.3, 0.6, 0.9, 1.2, and 1.5) w/v%

The rheological properties and filtration characteristics were obtained using a Fann VG meter and dead-weight hydraulic filter press from Fann Instrument Company (Houston, Texas). The No. 50 Whatman filter paper was used in the filtration experiment. The mud samples were analyzed for thermal stability by putting them into a stainless steel aging cell and hot-rolling them in a roller oven for 16 h.

2.6. Effects of Additive on Base Drilling Mud. *2.6.1. Rheological Parameters.* The drilling mud samples were prepared following the API guidelines,[39] and standard formulations were used to calculate the rheological parameters. Measurement of these parameters was conducted using a Fann VG meter, Fann Instrument Company (Houston, Texas). The mud gel strength depicts the ability of the fluid to suspend cuttings in the static condition.[40] The IG and FG were measured after 10 s and 10 min, respectively, at 3 rpm.

2.6.2. Static Filtration Test. As per guideline API 13B-1, a stainless steel filter cell from FANN Instruments Company, USA was used to test the static API filtration loss using grade 50 Whatman filter paper.[41] Data were collected at room temperature at a differential pressure of 100 psi. This test is vital to assessing the applicability of HACC as the drilling mud additive. After 30 min, the filtration loss volume was measured in milliliters (mL). The tests were repeated three times for each sample, and the average is reported to minimize the experimental error.

2.6.3. Thermal Stability of the Prepared Drilling Mud. The hot roller oven test is a classical test to assess the thermal stability of drilling mud formulations. The sample is put in the oven at various set temperatures for 16 h. The rheological characteristics of the high-performance drilling mud samples were compared in pre- and post-thermal conditions to evaluate the stability of the samples after aging. In the case of thermal degradation, the rheological properties such as PV, YP, and AV tend to decrease.

2.6.4. Shale Recovery Test. The shale recovery test is conducted using a hot roller oven. The mixture of 400 mL of mud sample and 20 g (w_0) of shale cuttings is kept in the hot roller oven for 16 h at 100 °C. After the set time, the cutting residues were sieved (60 mesh size) and rinsed in water. The remaining cuttings on the sieve were further dried at 100 °C for six hours to obtain a uniform weight (w_1) of the cuttings. The cuttings (w_1) in the fresh water were further hot rolled for 2 h at 100 °C. These hot-rolled cuttings were dried at 100 °C for 6 h again, and the weight (w_2) was noted down. These sequential weights were used to obtain the primary and secondary recovery percentages as presented in eqs 1 and (2).

$$\text{Primary recovery percentage } (\%R_1) = w_1/w_0 \times 100\% \quad (1)$$

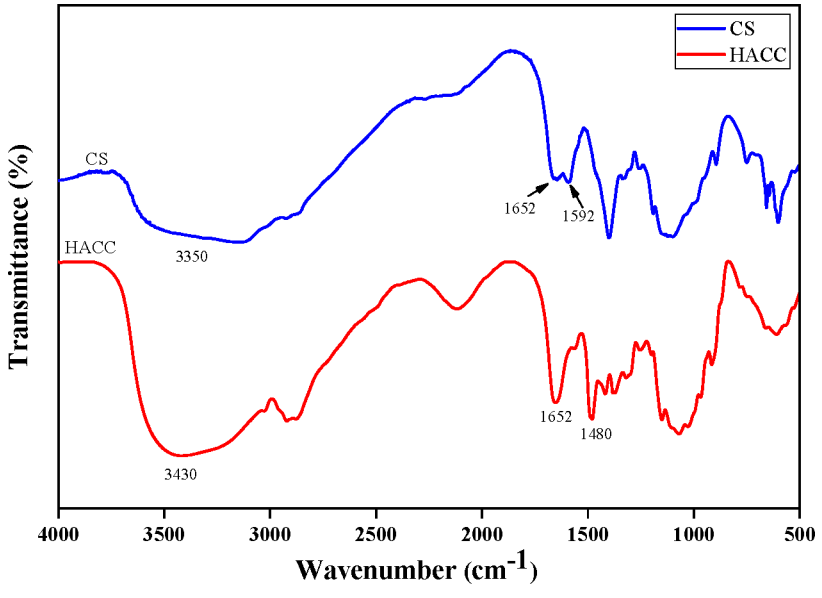

Figure 3. FTIR spectra of chitosan and HACC.

https://doi.org/10.1021/acsomega.4c01632
ACS Omega 2024, 9, 21365−21377

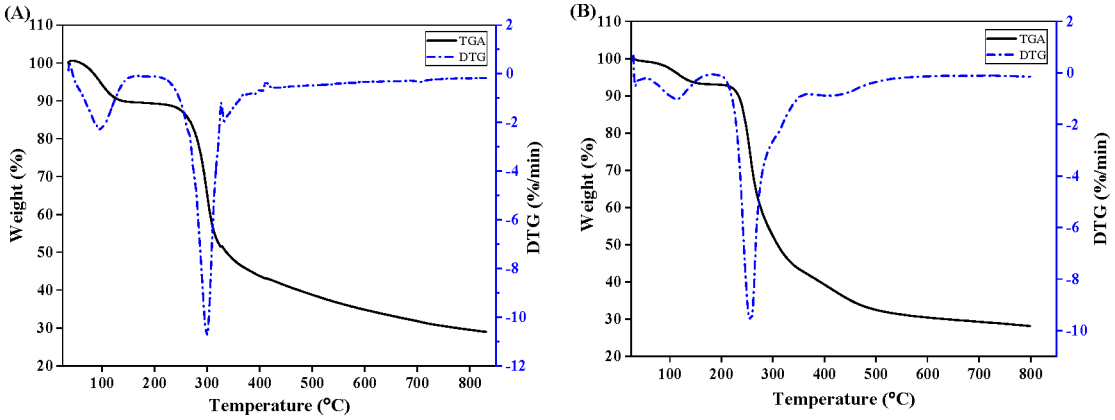

Figure 4. TGA and DTG analysis of (A) chitosan and (B) HACC.

$$\text{Secondary recovery percentage } (\%R_2) = w_2/w_0 \times 100\% \quad (2)$$

2.7. Mechanism Evaluation. *2.7.1. Characterization of HACC/Bentonite Composites.* To evaluate the interaction between the inhibitor and bentonite, different HACC/bentonite composites were prepared. Bentonite dispersions were prepared by continuously stirring for 24 h in distilled water. Along with bentonite, the concentration of HACC was varied from 0.3 to 1.5 w/v%, and the mixture was stirred continuously for an additional 24 h. After that, the prepared sample was centrifuged at 8000 rpm for 15 min. The precipitate was washed with distilled water multiple times to remove unabsorbed polymer and dried at 55 °C.[42,43]

The characterization of the composites was done by FTIR and XRD. Infrared spectra of the samples were recorded on a PerkinElmer Spectrum Two FTIR instrument (USA). XRD analysis was performed on a Rigaku SmartLab X-ray diffractometer; the samples were subjected to the following settings: 40 kV and 40 mA at 1.54059 Å with Cu Kα radiation to determine the XRD. The appropriate amount of material was spread out on a sample stage, and at a scan rate of 1° min^{-1}, the relative intensity was measured in the scattering range (2θ°) of 3−15°.

2.7.2. Zeta Potential Test. The zeta potential is the difference in the potential between the bulk solution and the solid surface. While the particles are suspended in the aqueous phase, the electrical charge of the particle is measured. Samples of HACC/bentonite composites were prepared, and 1 mL of the sample was added to 100 mL of deionized water. Each solution was further mixed with the help of a mechanical stirrer. The zeta potential of the different concentrations of HACC/bentonite composites was measured with the help of an Anton Paar Litesizer 500 through the electrophoresis method at 25 °C. All of the measurements were repeated three times for each sample.

3. RESULTS AND DISCUSSION

3.1. FTIR Spectroscopy. The FTIR spectra of HACC and chitosan are shown in Figure 3. The broad characteristic peak of CS and HACC at 3350 and 3430 cm^{-1} is attributed to the axial stretching of O−H and N−H_2 bonds and intermolecular hydrogen bonds.[37,44,45] The characteristic peaks at 1652 and 1592 cm^{-1} correspond to the amide I and amine II (bending vibration of −NH_2) absorption bands of chitosan, respectively.[37] For the FTIR spectrum of quaternized chitosan, the adsorption band at 1592 cm^{-1} almost disappeared, indicating that N-alkylation in chitosan occurred. A new band, observed at 1480 cm^{-1}, is attributed to the methyl groups of the ammonium; this corresponds to quaternized ammonium chloride due to C−H bond vibrations in CH_3 groups.[44,46,47] These results indicate that HACC was successfully synthesized.

3.2. TGA Analysis. TGA is a thermal analysis technique used to study the behavior of materials under varying temperature conditions. It measures the change in weight of a sample as it is heated or cooled under a controlled atmosphere. The weight change is typically due to processes such as decomposition, oxidation, reduction, or evaporation. In Figure 4, the TGA and DTG graphs of chitosan and HACC are shown. It shows that, within the temperature range of 30−200 °C, the first degradation occurs, which is caused by moisture loss and evaporation of bonding water.[32,48] This indicates a mass loss of about 11% for chitosan and 7% for HACC. It continued to decompose as a result of further thermal degradation, resulting in dehydration of the saccharide rings, depolymerization, and decomposition of the side chains.[44] The second degradation occurs at 200−300 °C indicating a mass loss of 60% for chitosan and 50% for HACC. The third and final degradation occurs within 300−800 °C indicating a mass loss of 70% for chitosan and 71% for HACC. As a result of the introduction of the new groups (quaternary ammonium group) to chitosan, the hydrogen bond of CS was broken.[44] From the results, it can be interpreted that HACC has a lower decomposition temperature than CS. Using TGA analysis, it was found that HACC was thermally stable and that the additive itself was not destroyed below 200 °C. This expanded the applicability of HACC, implying that the additive structure was stable at this temperature.

3.3. FESEM Analysis. Utilizing the FESEM analysis, the surface morphology of both CS and HACC is evaluated; it shows distinct morphological differences when comparing the synthesized additive with chitosan, as illustrated in Figure 5(A,B). The image shown has 15,000 times magnification. It is observed that chitosan has a more sloughy structure and the synthesized product has cylindrical and irregular shapes adsorbed onto a sloughy surface. Synthesizing chitosan brings about observable modifications in the surface morphology of HACC.

3.4. EDX Analysis. The EDX spectra of chitosan and HACC showed that chitosan has elemental peaks for carbon (C), oxygen (O), and nitrogen (N). HACC has shown elemental peaks for chlorine (Cl) as well as carbon, oxygen,

https://doi.org/10.1021/acsomega.4c01632
ACS Omega 2024, 9, 21365−21377

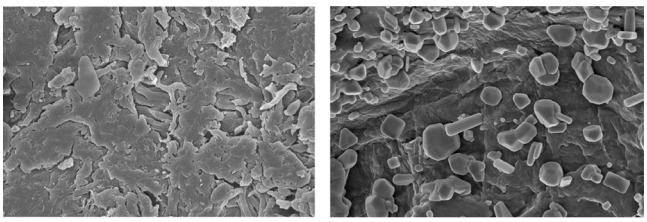

(A) (B)

Figure 5. FESEM images of (A) chitosan and (B) HACC.

Table 4. Elemental Analysis of Chitosan and HACC

Sl No.	Compound	Elements	Weight%
1	Chitosan	C	42.71
		N	11.46
		O	45.83
2	HACC	C	39.78
		N	10.42
		O	30.31
		Cl	19.49

and nitrogen. Therefore, it confirms the presence of amide functional group (NH_2) in both the compound and also the presence of chlorine in HACC. The detailed EDX analysis of chitosan and HACC was done, and it is shown in Figure 6 and Table 4.

3.5. Effect of HACC on the Rheological Properties of Drilling Mud. After obtaining the results of all the rheological properties such as PV, AV, YP, IG, and FG the comparison of rheological fluid formulations base mud 1, 2, and 3 at different concentrations of PEI and HACC is discussed and shown in graphs.

PV is the measure of a fluid's internal resistance to flow, determined by the type, quantity, and size of solids, representing the resistance beyond the YP and influenced by solid concentration, size, and the viscosity of the fluid phase.[40,49,50] The PV of the fluid formulations base mud 1, 2, and 3 at different concentrations of HACC are compared with a conventional additive PEI, and it is shown in Figure 7(A), (B), & (C), respectively. In Figure 7(A), on adding different concentrations of HACC to the base mud, the PV tends to increase from 7.5 to 9.5 cP, whereas on adding PEI to the base mud the PV tends to decrease initially (to 6.5 cP) and then increases as the concentration of additive increases. As shown in the graph, the trend of the PV graph remains similar for both the conventional shale inhibitor and the synthesized additive.

The YP at different concentrations of the additives is shown in Figure 8(A–C). It refers to the minimum stress needed to move the fluid.[50] For the three base muds as the concentration of XG increases, the YP value increases as seen in Figure 8. Similar to PV the YP value also initially decreases to 11 lb/100 ft^2 from 13 lb/100 ft^2 for base mud 1 on adding 0.3 w/v% PEI, whereas the YP increases to 15 lb/100 ft^2 on adding 0.3 w/v% HACC. Further on adding more additives the YP increases. A similar trend continues for base mud 2 and 3. An increase in YP results in the cleaning of the wellbore and also an increase in the equivalent circulation density.[40]

PV and YP are combined to determine AV; as a result, if either or both increase, AV will increase as well.[49] The AV at different concentrations of the additives is shown in Figure 9(A–C) for base mud 1, 2, and 3, respectively. On adding different concentrations of HACC and PEI the AV varies, and it increases with the increase in the concentration of additives; the trend of the conventional additive and the synthesized additive remains similar for all the base mud.

The gel strength of the fluid formulations was measured at a low shear rate of 3 rpm at a time interval of 10 s and 10 min for IG and FG, respectively. It is measured in lb/100 ft^2. The IG and the FG of the different drilling mud formulations are shown in Figure 10(A–C). The results shown in the figure show a progressive gel strength, which means the value of FG is much higher than IG; it suggests that the drilling mud strengthens as time progresses. On maintaining a progressive gel strength in the drilling mud the cuttings remain suspended even when the circulation is stopped. Also, after the hot rolling process, the drilling mud exhibits similar progressive gel strength, which suggests that the mud formulations are stable.[40,51]

For base mud 1, the gel strength increased from 7 lb/100 ft^2 in 10 s to 9.5 lb/100 ft^2 in 10 min. On adding 0.3 w/v% HACC the IG decreased by a small value, whereas the FG remained the same as the base mud, and on adding more concentrations of the additive the gel strength continued to increase. IG on adding 0.3 w/v% PEI is more, i.e., 11 lb/100 ft^2 compared to 6 lb/100 ft^2 for HACC. A similar trend follows for the fluid formulations of base mud 2 (Figure 10(B)). For the mud formulations of base mud 3 at different concentrations of additives, it is observed in Figure 10(C) that the gel strength properties of base mud 3 are comparatively higher; this is due to the increase in viscosity of the polymeric

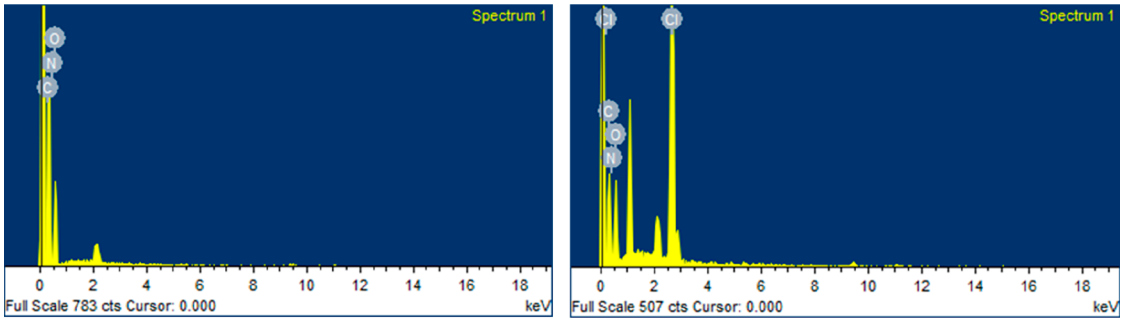

(A) (B)

Figure 6. EDX analysis of (A) chitosan and (B) HACC.

https://doi.org/10.1021/acsomega.4c01632
ACS Omega 2024, 9, 21365−21377

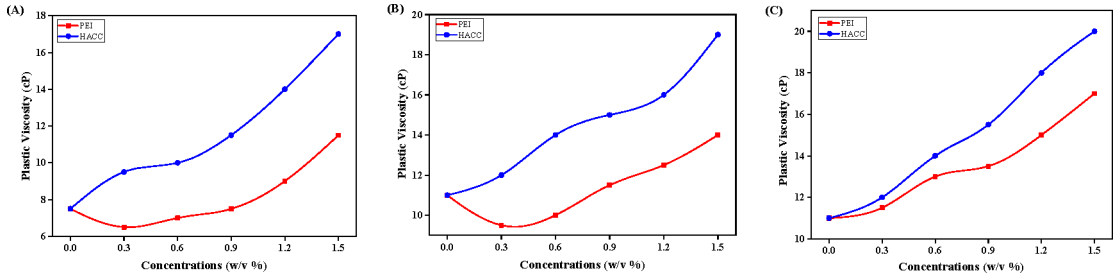

Figure 7. Comparison of the PV of the fluid formulations: (A) Base mud 1, (B) Base mud 2, and (C) Base mud 3 at different concentrations of PEI and HACC.

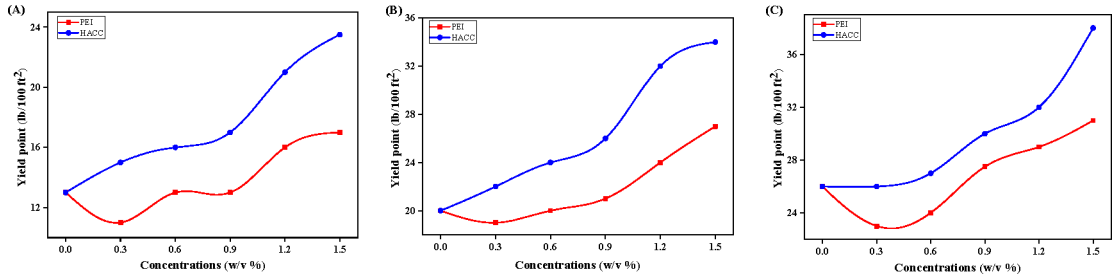

Figure 8. Comparison of the YP of the fluid formulations: (A) Base mud 1, (B) Base mud 2, and (C) Base mud 3 at different concentrations of PEI and HACC.

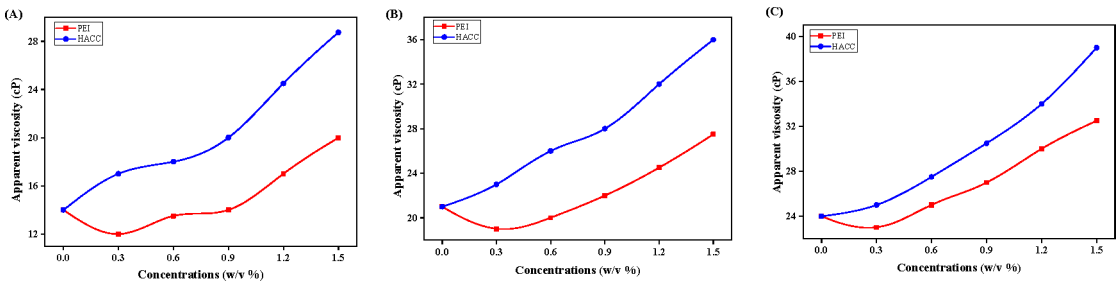

Figure 9. Comparison of the AV of the fluid formulations: (A) Base mud 1, (B) Base mud 2, and (C) Base mud 3 at different concentrations of PEI and HACC.

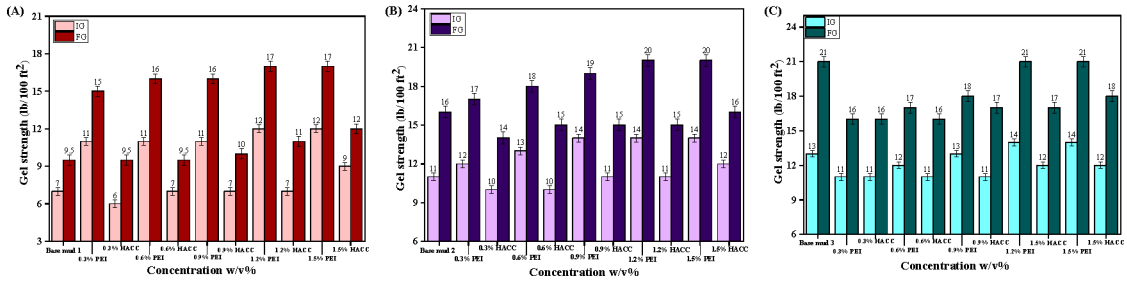

Figure 10. Comparison of the gel strength of the fluid formulations: (A) Base mud 1, (B) Base mud 2, and (C) Base mud 3 at different concentrations of PEI and HACC.

solutions. From the results, we can conclude that HACC shows better progressive gel strength compared to PEI.

3.6. Effect of HACC on the Static Filtration Properties.

The primary objective of drilling mud is to reduce filtration and, hence, minimize fluid loss. Figure 11(A–C) represents the results of static filtration loss for various drilling mud formulations. The fluid loss for base mud formulations 1, 2, and 3 is measured at 21, 19, and 17 mL, respectively. A slight decrease in fluid loss is observed with an increasing concentration of XG in the base fluid. Incorporating 0.3 w/v % of HACC into base mud 1 results in a 42.86% reduction in fluid loss, significantly outperforming the 10% reduction by PEI. Similarly, for base mud formulations 2 and 3, the addition of 0.3 w/v% HACC results in a substantial 47.36% and 47.06% decrease in filtration loss, while PEI achieves only a 10.5% and 5.9% reduction in fluid loss, respectively. Therefore it is evident that the synthesized additive has better fluid loss control in comparison to PEI.

The graphical representation reinforces the effectiveness of HACC over PEI in fluid loss control, demonstrating a more pronounced reduction as higher additive concentrations are introduced. It is noteworthy that during the static filtration

https://doi.org/10.1021/acsomega.4c01632
ACS Omega 2024, 9, 21365−21377

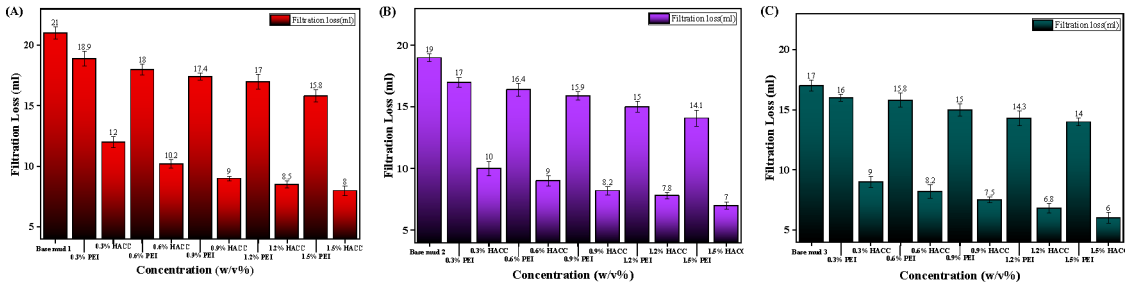

Figure 11. Static filtration loss of (A) Base mud 1, (B) Base mud 2, and (C) Base mud 3 at different concentrations of PEI and HACC.

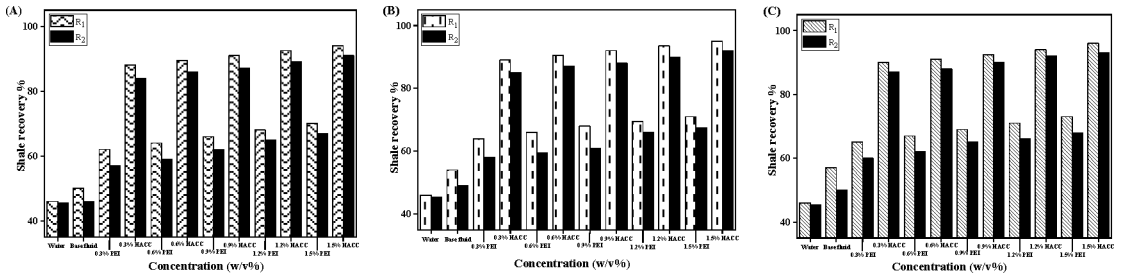

Figure 12. Primary and secondary shale cutting recovery rates of (A) Base mud 1, (B) Base mud 2, and (C) Base mud 3 at different concentrations of PEI and HACC post hot rolling at 100 °C.

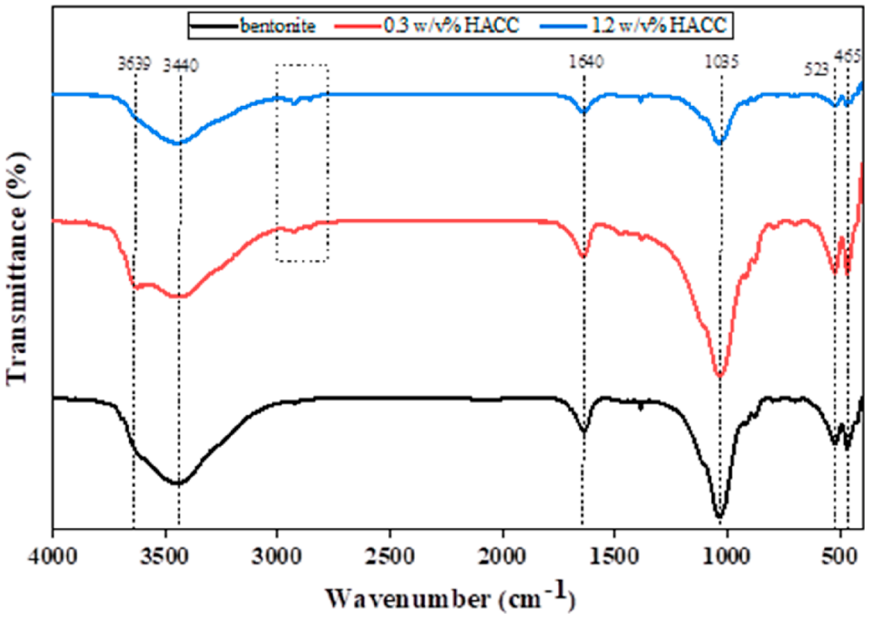

Figure 13. FTIR analysis of bentonite and HACC/bentonite composites.

experiment, both additives yielded comparatively thin filter cakes. This characteristic is essential for shale formations, as thick filter cakes are undesirable as they reduce polymer concentration in the filtrate and also the protective covering for shale inhibition.

3.7. Effect of HACC on Shale Recovery. One of the important factors to consider when understanding and mitigating well instability is drilling mud design.[52] This process requires determining the shale recovery for drilling mud. As the studied shale samples easily disperse and hydrate in water, thorough analysis and optimization of drilling mud compositions are required to ensure their stability and efficiency. After 16 h of hot rolling the aging cell containing the drilling mud and shale cuttings in the hot roller oven, the primary and secondary recovery percentages of the shale cuttings denoted as $\%R_1$ and $\%R_2$, respectively, were determined. The $\%R_1$ and $\%R_2$ of water are found to be 46% and 45.5%. The shale recovery of our three base fluid formulations base mud 1, 2, and 3 increases by a minor value as the concentration of the XG increases from 0.3% to 0.5% (50, 54, and 57%). After the addition of different amounts of PEI and HACC to the base fluids, the shale recovery of the formulation seems to vary, along with the different concentrations of additives. In Figure 12, it is observed that the shale recovery increases as the concentration of the synthesized additive increases for each respective base mud. Upon comparison with PEI, the addition of just 0.3% of the synthesized additive to the three base mud systems results in a significant 91.3, 93.47, and 95.65% increase

https://doi.org/10.1021/acsomega.4c01632
ACS Omega 2024, 9, 21365−21377

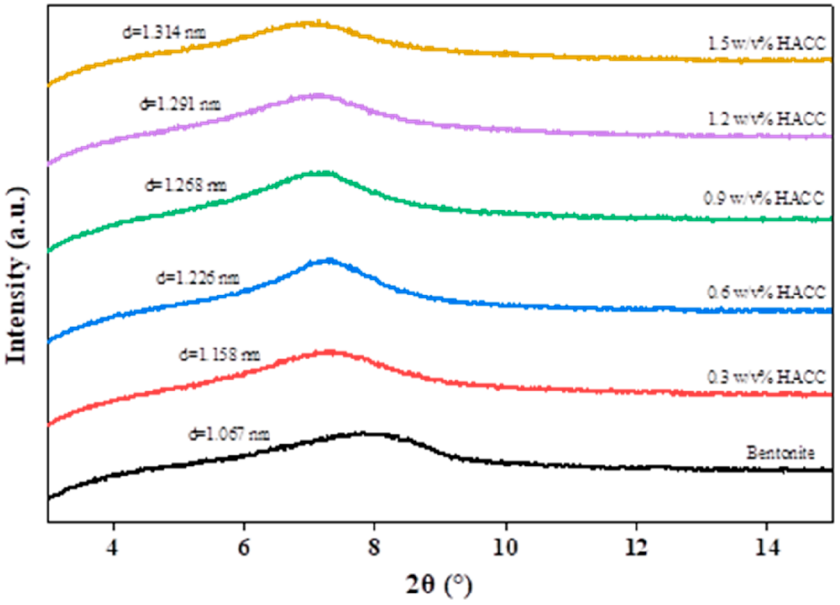

Figure 14. XRD patterns of bentonite and modified bentonite at different concentrations of HACC.

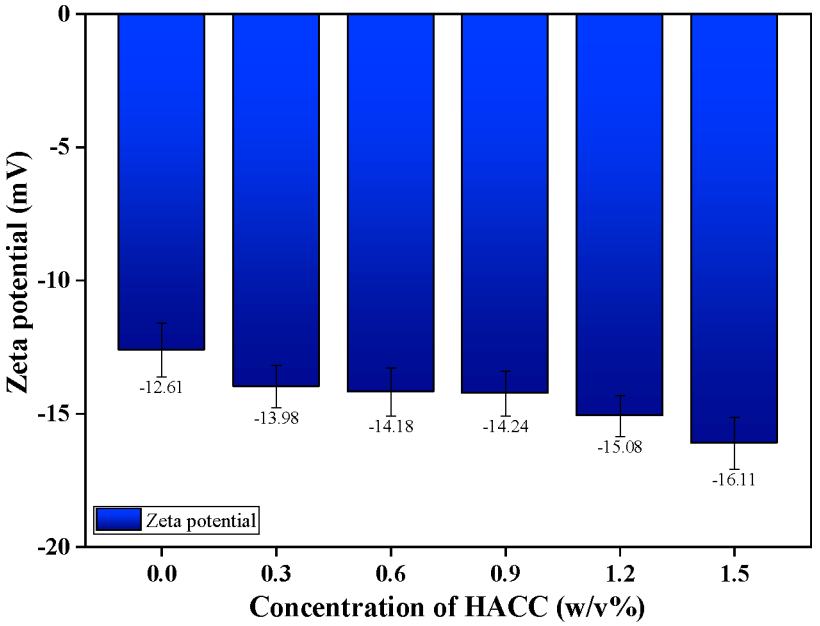

Figure 15. Zeta potential of bentonite at different concentrations of HACC.

in recovery percentage when compared with water, while the incorporation of 0.3 w/v% of PEI leads to only a 34.78, 39.13, and 41.30% enhancement in recovery. The $\%R_1$ at each concentration of HACC shown is significantly above 88%, which indicates that it has a better ability to inhibit shale swelling. Similarly, the shale recovery percentage varies with an increase in the concentration of the additives. Compared to the conventional shale inhibitor, a good inhibiting property was observed by HACC, which reduced the swelling or hydration of the shale cuttings efficiently.

3.8. Inhibition Mechanism Analysis. *3.8.1. FTIR Analysis.* The FTIR analyses of bentonite and HACC/bentonite composites are shown in Figure 13. The peaks of bentonite demonstrated the characteristic bands of montmorillonite. The peak at 3639 cm^{-1} indicates a stretching band in the octahedral sheet for Al−O−H. 3440 and 1640 cm^{-1} are related to the deformation and stretching of the O−H bond of physisorbed water. The strong absorption peak at 1035 cm^{-1} can be associated with the Si−O antisymmetric stretching vibration of the structural lattice, and the peaks at 523 and 465 cm^{-1} can be attributed to the Si−O−Mg/Fe deformation. Two additional peaks at 2926 cm^{-1} to 2870 cm^{-1} are observed in the HACC/bentonite composite spectrum, which suggests the C−H stretching vibration of the alkyl group and thereby confirms the interaction between HACC and bentonite. Moreover, the characteristic peaks at 3440 and 1640 cm^{-1} are also weakened, indicating the inhibition of shale hydration due to the interaction of HACC with bentonite. The cation exchange phenomenon occurs when the additive adsorbs and intercalates between the clay layers through hydrogen bonding and electrostatic attraction indicating a reduction in interlayer water in bentonite.[53−55] Here, it is worth noting that only two

https://doi.org/10.1021/acsomega.4c01632
ACS Omega 2024, 9, 21365−21377

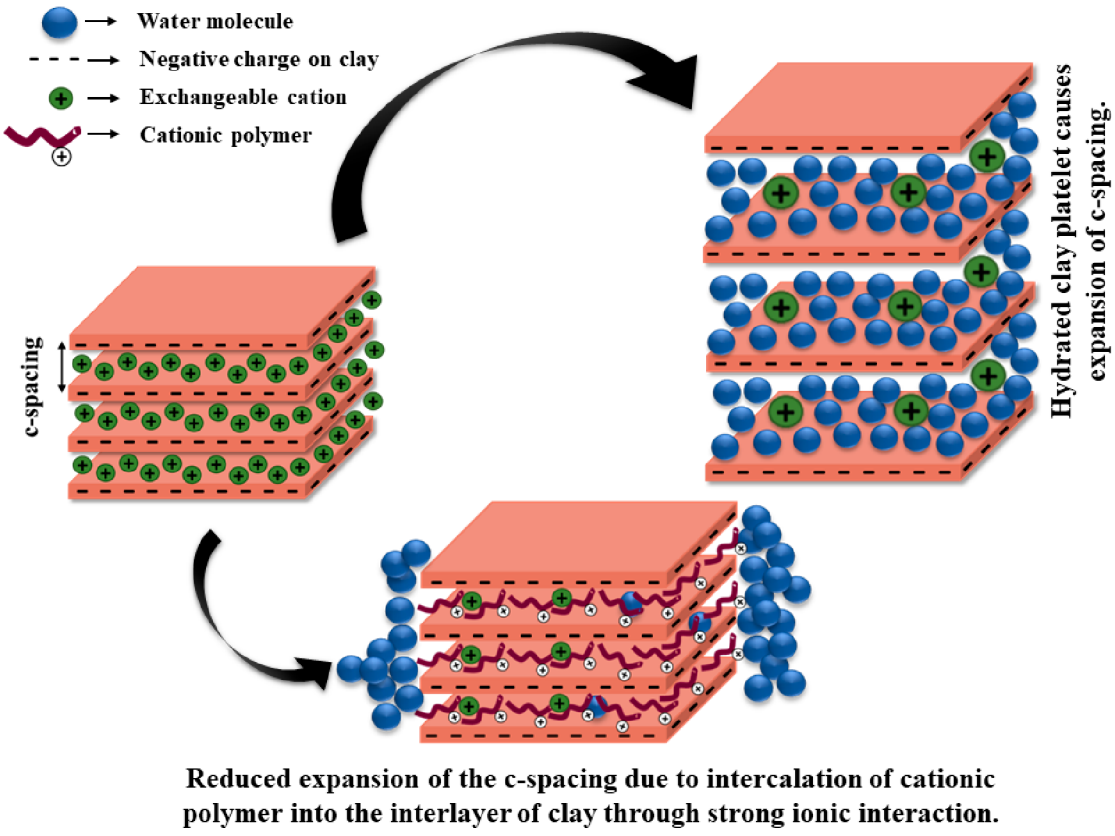

Figure 16. Schematic representation of the shale inhibition mechanism.

HACC/bentonite composites are presented. The characteristic peak remains consistent across different concentrations, with variations in peak intensity observed based on concentration.

3.8.2. XRD Analysis. Contact with water usually induces both crystalline swelling and osmotic swelling in clay, causing an expansion of bentonite interlayer spacing. XRD is a commonly employed technique to evaluate changes in the bentonite interlayer spacing. The XRD patterns of bentonite and HACC/bentonite composites are shown in Figure 14. The interlayer spacing (d) is determined by Bragg's equation ($n\lambda = 2d \sin \theta$). The interlayer spacing of bentonite is found to be 1.067 nm. In the modified samples, the peaks shifted to the lower 2θ values, which indicated the expansion of interlayer space. On adding 0.3 w/v% HACC to bentonite, the spacing increased to 1.158 nm, which suggests the intercalation of the additive. For various concentrations of HACC, the interlayer spaces increased from 1.226 to 1.314 nm. It can be inferred that HACC can effectively intercalate into clay interlayer, thus inhibiting the clay swelling.[42,43,54,55]

3.8.3. Zeta Potential Analysis. The zeta potential measurement is another standard way to investigate the mechanism of the interaction between clay particles and shale inhibitors. An isomorphous substitution in the octahedral layer causes the clay particles to naturally carry a negative charge. The magnitude of the zeta potential indicates the stability of a sample. The high zeta-potential value suggests a higher degree of repulsion, indicating the suspension of particles as desirable for drilling fluid. When the zeta potential value drops, the tendency of the solid particle aggregation increases and makes the fluid system more unstable. Figure 15 presents the zeta potential of dispersed bentonite and HACC/bentonite composites. It is observed that the addition of HACC increases the magnitude of the zeta potential. Additionally, it can also be seen that the difference in zeta potential from 0.3−0.9 w/v% is not very significant. However, as the concentration increases from 0.9 to 1.2 w/v%, there is significant change in zeta potential. This change can be attributed to an increased possibility of particle suspension.[56,57]

3.9. Shale Inhibition Mechanism. The interlayers of the clay mineral contain sodium and calcium ions, which balance out the negative charge of the clay mineral.[58] Clay swelling takes place due to the hydration of cations, leading to the expansion of clay platelets. The cation exchange phenomenon occurs when HACC is introduced, and the additive adsorbs and intercalates between the clay layers through hydrogen bonding and electrostatic attraction. Since clay particles are electronegative, the most efficient shale inhibitor is usually electropositive, following the fundamental electrical law that states that opposing charges attract.[37] Figure 16 shows a schematic representation explaining the interaction between HACC and clay particles as well as shale formation. HACC is a polyampholyte, which contains amine groups along with ammonium cations; the amine groups will be protonated and converted into ammonium ions when dispersed in water. These ammonium ions would firmly adsorb via hydrogen bonding and electrostatic interaction on the surface of clay particles.[59,60] Molecules will intercalate into the clay platelets, resulting in a reduction in the interlayer spacing between clay particles. This suggests that the ability of clay particles to hydrate and swell has been reduced. The polyampholyte additive is easily adsorbed onto the negatively charged surface of the shale formation. The invasion of water into the shales would be significantly reduced, as observed in the above shale recovery test. After modification of chitosan, the additive

https://doi.org/10.1021/acsomega.4c01632
ACS Omega 2024, 9, 21365−21377

inhibits swelling by intercalation as well as by adsorption onto the clay surface, which improves shale stability.

3.10. Optimized Drilling Fluid Formulation. The optimization of the rheological properties (PV, YP, AV, IG, and FG) is crucial to achieve efficient operational drilling parameters such as increased rate of penetration (ROP) and better suspension of cuttings. Past studies suggest that the acceptable range of PV, AV, and YP are 10 to 20 cP, 25 to 35 cP, and 12 to 36 lb/100 ft^2, respectively, for efficient drilling in shale formation.[17,25,61] These criteria are found to be satisfied by 8 combinations of the HACC additions to three base fluids (refer to Supporting Information). Additionally, the increasing concentration of HACC in base fluids increases progressive gel strength, reduces the filtrate loss, and increases the shale recovery. Furthermore, the zeta potential results show a significant increase at the transition of 0.9 w/v% to 1.2 w/v% addition of HACC in the bentonite suggesting increased possibility of particle suspension. Overall, it can be inferred that 1.2 w/v% in the base fluids is better suited for the drilling operation in shale formation.

4. CONCLUSION

A novel shale inhibitor, chitosan-*N*-(2-hydroxyl)-propyl trimethylammonium chloride, was synthesized to use as an additive for water-based drilling fluids. The synthesized chitosan derivative was characterized by using different techniques and tested for its suitability as a drilling mud additive. Standard drilling fluid tests for filtration and rheological characterization were conducted to evaluate its performance as an additive. Overall, HACC demonstrated better efficiency than PEI in the context of shale hydration, clay swelling, and filtration loss.

i. The rheological and filtration properties show similar trends for the conventional additive and the synthesized chitosan-based additive.

ii. The addition of 0.3 w/v% of HACC into base mud 1 resulted in a 42.86% reduction in the fluid loss while the same concentration of PEI only exhibited a 10% reduction. Similar results were also exhibited by other concentrations of additives where HACC outperforms PEI. Therefore, it can be inferred that HACC is a better fluid loss control agent than PEI.

iii. After the hot-rolling process, the rheological and filtration properties of chitosan derivative remain almost similar indicating its stability and suitability for the drilling operations.

iv. The primary recovery percentage at different concentrations of HACC is found to be significantly above 88%, which shows its shale inhibition characteristics.

v. The addition of 0.3 w/v% of the synthesized additive to the three base mud systems resulted in increased recovery percentages by 91.3, 93.47, and 95.65%, while 0.3 w/v% of PEI addition only resulted in a 34.78, 39.13, and 41.30% increase in recovery percentages. This result shows that HACC is better suited for shale drilling operations in comparison to PEI.

vi. HACC intercalates into clay platelets, reducing the interlayer spacing between particles and preventing clay from hydrating and swelling. This mechanism of inhibition is evaluated by X-ray diffraction, FTIR, and zeta potential analysis.

vii. The optimum concentration for HACC addition is found to be 1.2 w/v% for three types of base fluids.

In conclusion, HACC can be used to drill shale gas formations successfully due to its excellent shale inhibitor properties in drilling fluids. Due to its various potential benefits, such as improved rheological properties and reduced filtration, along with its cost-benefit and abundance in raw materials, it is a good additive for water-based drilling mud.

■ ASSOCIATED CONTENT

Supporting Information

The Supporting Information is available free of charge at https://pubs.acs.org/doi/10.1021/acsomega.4c01632.

Rheological properties comparison for optimization of drilling fluid formulation (PDF)

■ AUTHOR INFORMATION

Corresponding Author

Vinay Kumar Rajak − *Department of Petroleum Engineering, IIT (ISM) Dhanbad, Dhanbad, Jharkhand 826004, India;* orcid.org/0000-0002-4384-5295; Email: vinayrajak@iitism.ac.in

Authors

Amolina Doley − *Department of Petroleum Engineering, IIT (ISM) Dhanbad, Dhanbad, Jharkhand 826004, India*

Vikas Mahto − *Department of Petroleum Engineering, IIT (ISM) Dhanbad, Dhanbad, Jharkhand 826004, India;* orcid.org/0000-0002-9543-4164

Raj Kiran − *Department of Petroleum Engineering, IIT (ISM) Dhanbad, Dhanbad, Jharkhand 826004, India;* orcid.org/0000-0003-0782-5438

Rajeev Upadhyay − *Department of Petroleum Engineering, IIT (ISM) Dhanbad, Dhanbad, Jharkhand 826004, India*

Complete contact information is available at: https://pubs.acs.org/10.1021/acsomega.4c01632

Notes

The authors declare no competing financial interest.

■ ACKNOWLEDGMENTS

The authors would like to thank Indian Institute of Technology (Indian School of Mines) Dhanbad for providing the required laboratory facilities and financial support to carry out our research work. We would also like to acknowledge DST SERB for the financial support provided under the research grant MTR/2023/000822.

■ NOMENCLATURE

KCl - Potassium chloride
HACC - Chitosan-*N*-(2-hydroxyl)-propyl trimethylammonium chloride
TGA - Thermogravimetric analysis
FTIR - Fourier transform infrared
EDX - Energy-dispersive X-ray
FESEM - Field-emission scanning electron microscopy
XG - Xanthan gum
PEI - Polyethylenimine
CS - Chitosan
NaOH - Sodium hydroxide
XRD - X-ray diffraction
XRF - X-ray fluorescence

https://doi.org/10.1021/acsomega.4c01632
ACS Omega 2024, 9, 21365−21377

CEC - Cation exchange capacity
API - American Petroleum Institute
PV - Plastic viscosity
YP - Yield point
AV - Apparent viscosity
FG - Final gel strength
IG - Initial gel strength
DTG - Derived thermogravimetric

REFERENCES

(1) Ross, D. J. K.; Marc Bustin, R. The Importance of Shale Composition and Pore Structure upon Gas Storage Potential of Shale Gas Reservoirs. *Mar. Pet. Geol.* **2009**, *26* (6), 916−927.
(2) Hart, B. S.; Macquaker, J. H. S.; Taylor, K. G. Mudstone ("shale") Depositional and Diagenetic Processes: Implications for Seismic Analyses of Source-Rock Reservoirs. *Interpretation* **2013**, *1* (1), B7−B26.
(3) Karpiński, B.; Szkodo, M. Clay Minerals − Mineralogy and Phenomenon of Clay Swelling in Oil & Gas Industry. *Adv. Mater. Sci.* **2015**, *15* (1), 37−55.
(4) Brigatti, M. F.; Galán, E.; Theng, B. K. G. Chapter 2 - Structure and Mineralogy of Clay Minerals. *Dev. Clay Sci.* **2013**, *5*, 21−81.
(5) Rana, A.; Arfaj, M. K.; Saleh, T. A. Advanced Developments in Shale Inhibitors for Oil Production with Low Environmental Footprints − A Review. *Fuel* **2019**, *247* (March), 237−249.
(6) Anderson, R. L.; Ratcliffe, I.; Greenwell, H. C.; Williams, P. A.; Cliffe, S.; Coveney, P. V. Clay Swelling - A Challenge in the Oilfield. *Earth-Science Rev.* **2010**, *98* (3−4), 201−216.
(7) Saleh, T. A.; Rana, A.; Arfaj, M. K. Graphene Grafted with Polyethyleneimine for Enhanced Shale Inhibition in the Water-Based Drilling Fluid. *Environ. Nanotechnology, Monit. Manag.* **2020**, *14* (July), No. 100348.
(8) Rana, A.; Arfaj, M. K.; Saleh, T. A. Advanced Developments in Shale Inhibitors for Oil Production with Low Environmental Footprints − A Review. *Fuel* **2019**, *247* (Feb), 237−249.
(9) Mohiuddin, M. A.; Khan, K.; Abdulraheem, A.; Al-Majed, A.; Awal, M. R. Analysis of Wellbore Instability in Vertical, Directional, and Horizontal Wells Using Field Data. *J. Pet. Sci. Eng.* **2007**, *55* (1−2), 83−92.
(10) Ahmed, H. M.; Kamal, M. S.; Al-Harthi, M. Polymeric and Low Molecular Weight Shale Inhibitors: A Review. *Fuel* **2019**, *251* (March), 187−217.
(11) An, Y.; Yu, P. A Strong Inhibition of Polyethyleneimine as Shale Inhibitor in Drilling Fluid. *J. Pet. Sci. Eng.* **2018**, *161*, 1−8.
(12) Li, X.; Jiang, G.; Shen, X.; Li, G. Poly- l -Arginine as a High-Performance and Biodegradable Shale Inhibitor in Water-Based Drilling Fluids for Stabilizing Wellbore. *ACS Sustain. Chem. Eng.* **2020**, *8* (4), 1899−1907.
(13) Huang, X.; Shen, H.; Sun, J.; Lv, K.; Liu, J.; Dong, X.; Luo, S. Nanoscale Laponite as a Potential Shale Inhibitor in Water-Based Drilling Fluid for Stabilization of Wellbore Stability and Mechanism Study. *ACS Appl. Mater. Interfaces* **2018**, *10* (39), 33252−33259.
(14) Saki, Y.; Dinarvand, N.; Habibnia, B.; Shahbazi, K. Experimental Investigation of Possibility of Replacing Oil-Based Muds with Environmentally Friendly Water-Based Glycol Muds in Maroon Oil Field. *Soc. Pet. Eng. - Trinidad Tobago Energy Resour. Conf. 2010, SPE TT 2010* **2010**, *1*, 401−413.
(15) Jingyuan, M.; Boru, X.; Yuxiu, A. Advanced Developments in Low-Toxic and Environmentally Friendly Shale Inhibitor: A Review. *J. Pet. Sci. Eng.* **2022**, *208* (PC), No. 109578.
(16) Zhong, H. Y.; Qiu, Z. S.; Huang, W. A.; Cao, J.; Wang, F. W.; Zhang, X. B. An Inhibition Properties Comparison of Potassium Chloride and Polyoxypropylene Diamine in Water-Based Drilling Fluid. *Pet. Sci. Technol.* **2013**, *31* (20), 2127−2133.
(17) Jain, R.; Mahto, V.; Sharma, V. P. Evaluation of Polyacrylamide-Grafted-Polyethylene Glycol/Silica Nanocomposite as Potential Additive in Water Based Drilling Mud for Reactive Shale Formation. *J. Nat. Gas Sci. Eng.* **2015**, *26*, 526−537.
(18) Liu, Y.; Zou, C.; Li, C.; Lin, L.; Chen, W. Evaluation of β-Cyclodextrin-Polyethylene Glycol as Green Scale Inhibitors for Produced-Water in Shale Gas Well. *Desalination* **2016**, *377*, 28−33.
(19) Clark, R.K.; Scheuerman, R.F.; Rath, H.; Van Laar, H.G. Polyacrylamide/Potassium-Chloride Mud for Drilling Water-Sensitive Shales. *SPE* **1976**, *28* (06), 719−727.
(20) Shi, X.; Wang, L.; Guo, J.; Su, Q.; Zhuo, X. Effects of Inhibitor KCl on Shale Expansibility and Mechanical Properties. *Petroleum* **2019**, *5* (4), 407−412.
(21) Ferreira, C. C.; Teixeira, G. T.; Lachter, E. R.; Nascimento, R. S. V. Partially Hydrophobized Hyperbranched Polyglycerols as Non-Ionic Reactive Shale Inhibitors for Water-Based Drilling Fluids. *Appl. Clay Sci.* **2016**, *132−133*, 122−132.
(22) Liu, S.; Mo, X.; Zhang, C.; Sun, D.; Mu, C. Swelling Inhibition by Polyglycols in Montmorillonite Dispersions. *J. Dispers. Sci. Technol.* **2004**, *25* (1), 63−66.
(23) Murtaza, M.; Kamal, M. S.; Mahmoud, M. Application of a Novel and Sustainable Silicate Solution as an Alternative to Sodium Silicate for Clay Swelling Inhibition. *ACS Omega* **2020**, *5* (28), 17405−17415, DOI: 10.1021/acsomega.0c01777.
(24) Reid, P. I.; Minton, R. C.; Twynam, A. SPE 24979 Field Evaluation of a Novel Inhibitive Water-Based Drilling Fluid for Tertiary Shales. *European Petroleum Conference*, Cannes, France, November, 1992; DOI: 10.2118/24979-MS.
(25) Guo, J.; Yan, J.; Fan, W.; Zhang, H. Applications of Strongly Inhibitive Silicate-Based Drilling Fluids in Troublesome Shale Formations in Sudan. *J. Petroleum Sci. Eng.* **2006**, *50*, 195−203, DOI: 10.1016/j.petrol.2005.12.006.
(26) Patel, A. D. Design and Development of Quaternary Amine Compounds: Shale Inhibition with Improved Environmental Profile. *Proc. - SPE Int. Symp. Oilf. Chem.* **2009**, *2*, 1007−1015.
(27) Cheung, R. C. F.; Ng, T. B.; Wong, J. H.; Chan, W. Y. Chitosan: An Update on Potential Biomedical and Pharmaceutical Applications. *Mar. Drugs* **2015**, *13* (8), 5156−5186, DOI: 10.3390/md13085156.
(28) Terkula Iber, B.; Azman Kasan, N.; Torsabo, D.; Wese Omuwa, J. A Review of Various Sources of Chitin and Chitosan in Nature. *J. Renew. Mater.* **2022**, *10* (4), 1097−1123.
(29) Shakeel, A.; Mudasir, A.; Saiqa, I. Chitosan: A Natural Antimicrobial Agent - A Review. *J. Appl. Chem.* **2014**, *2* (3), 493−503.
(30) Azmana, M.; Mahmood, S.; Hilles, A. R.; Rahman, A.; Arifin, M. A. B.; Ahmed, S. A Review on Chitosan and Chitosan-Based Bionanocomposites: Promising Material for Combatting Global Issues and Its Applications. *Int. J. Biol. Macromol.* **2021**, *185* (June), 832−848.
(31) Geng, Y.; Xue, H.; Zhang, Z.; Panayi, A. C.; Knoedler, S.; Zhou, W.; Mi, B.; Liu, G. Recent Advances in Carboxymethyl Chitosan-Based Materials for Biomedical Applications. *Carbohydr. Polym.* **2023**, *305*, No. 120555.
(32) Liu, Q.; Chen, J.; Yang, X.; Qiao, C.; Li, Z.; Xu, C.; Li, Y.; Chai, J. Synthesis, Structure, and Properties of N-2-Hydroxylpropyl-3-Trimethylammonium-O-Carboxymethyl Chitosan Derivatives. *Int. J. Biol. Macromol.* **2020**, *144*, 568−577.
(33) Yang, Z.; Peng, H.; Wang, W.; Liu, T. Crystallization Behavior of Poly(ε-Caprolactone)/Layered Double Hydroxide Nanocomposites. *J. Appl. Polym. Sci.* **2010**, *116* (5), 2658−2667.
(34) Xu, Y.; Du, Y.; Huang, R.; Gao, L. Preparation and Modification of N-(2-Hydroxyl) Propyl-3-Trimethyl Ammonium Chitosan Chloride Nanoparticle as a Protein Carrier. *Biomaterials* **2003**, *24* (27), 5015−5022.
(35) Qin, C.; Xiao, Q.; Li, H.; Fang, M.; Liu, Y.; Chen, X.; Li, Q. Calorimetric Studies of the Action of Chitosan-N-2-Hydroxypropyl Trimethyl Ammonium Chloride on the Growth of Microorganisms. *Int. J. Biol. Macromol.* **2004**, *34* (1−2), 121−126.
(36) Andreica, B. I.; Cheng, X.; Marin, L. Quaternary Ammonium Salts of Chitosan. A Critical Overview on the Synthesis and Properties Generated by Quaternization. *Eur. Polym. J.* **2020**, *139*, No. 110016.

https://doi.org/10.1021/acsomega.4c01632
ACS Omega 2024, 9, 21365−21377

(37) Doley, A.; Mahto, V.; Rajak, V. K.; Suri, A. Development of a High-Performance Drilling Fluid Additive for Application in Indian Shale Gas Formations. *Energy Fuels* **2023**, *37*, 12824.
(38) Mahto, V.; Sharma, V. P. Rheological Study of a Water Based Oil Well Drilling Fluid. *J. Pet. Sci. Eng.* **2004**, *45* (1−2), 123−128.
(39) API-13I. Recommended Practice for Laboratory Testing Drilling Fluids. *Am. Pet. Inst.* **2009**, *2008* (March), 191.
(40) Alakbari, F.; Elkatatny, S.; Kamal, M. S.; Mahmoud, M. Optimizing the Gel Strength of Water-Based Drilling Fluid Using Clays for Drilling Horizontal and Multi-Lateral Wells. *Soc. Pet. Eng. - SPE Kingdom Saudi Arab. Annu. Technol. Symp. Exhib. 2018, SATS 2018* **2018**, DOI: 10.2118/192191-ms.
(41) API. Recommend Practice for Field Testing Water-Based Drilling Fluids - 13B-1. In *ANSI/API Recommended Practice 13B-1;* API, 2017; *2008*, (March), p 121.
(42) Zhong, H.; Qiu, Z.; Huang, W.; Sun, D.; Zhang, D.; Cao, J. Synergistic Stabilization of Shale by a Mixture of Polyamidoamine Dendrimers Modified Bentonite with Various Generations in Water-Based Drilling Fluid. *Appl. Clay Sci.* **2015**, *114*, 359−369.
(43) Lei, M.; Huang, W.; Sun, J.; Shao, Z.; Wu, T.; Liu, J.; Fan, Y. Synthesis of Carboxymethyl Chitosan as an Eco-Friendly Amphoteric Shale Inhibitor in Water-Based Drilling Fluid and an Assessment of Its Inhibition Mechanism. *Appl. Clay Sci.* **2020**, *193* (May), No. 105637.
(44) Cai, J.; Dang, Q.; Liu, C.; Wang, T.; Fan, B.; Yan, J.; Xu, Y. Preparation, Characterization and Antibacterial Activity of O-Acetyl-Chitosan-N-2-Hydroxypropyl Trimethyl Ammonium Chloride. *Int. J. Biol. Macromol.* **2015**, *80*, 8−15.
(45) Tamer, T. M.; Hassan, M. A.; Omer, A. M.; Baset, W. M. A.; Hassan, M. E.; El-Shafeey, M. E. A.; Eldin, M. S. M. Synthesis, Characterization and Antimicrobial Evaluation of Two Aromatic Chitosan Schiff Base Derivatives. *Process Biochem.* **2016**, *51* (10), 1721−1730.
(46) Loubaki, E.; Ourevitch, M.; Sicsic, S. Chemical Modification of Chitosan By Glycidyl Trimethylammonium Chloride. *Eur. Polym. J.* **1991**, *27* (3), 311−317.
(47) Shagdarova, B.; Lunkov, A.; Il'ina, A.; Varlamov, V. Investigation of the Properties of N-[(2-Hydroxy-3-Trimethylammonium) Propyl] Chloride Chitosan Derivatives. *Int. J. Biol. Macromol.* **2019**, *124*, 994−1001.
(48) Yang, X.; Zhang, C.; Qiao, C.; Mu, X.; Li, T.; Xu, J.; Shi, L.; Zhang, D. A Simple and Convenient Method to Synthesize N-[(2-Hydroxyl)-Propyl-3-Trimethylammonium] Chitosan Chloride in an Ionic Liquid. *Carbohydr. Polym.* **2015**, *130*, 325−332.
(49) Razi, M. M.; Mazidi, M.; Razi, F. M.; Aligolzadeh, H.; Niazi, S. Artificial Neural Network Modeling of Plastic Viscosity, Yield Point, and Apparent Viscosity for Water-Based Drilling Fluids. *J. Dispers. Sci. Technol.* **2013**, *34* (6), 822−827.
(50) Chilingarian, G. V.; Alp, E.; Caenn, R.; Al-Salem, M.; Uslu, S.; Gonzales, S.; Dorovi, R. J.; Mathur, R. M.; Yen, T. F. Drilling Fluid Evaluation Using Yield Point-Plastic Viscosity Correlation. *Energy Sources* **1986**, *8* (2−3), 233−244.
(51) Ye, A.; Kleinguetl, K.; Kulkarni, S.; et al. Gel Strength Measurement for Drilling Fluid: Reform of Gel Microstructure. *Am. Assoc. Drill. Eng.* **2015**, 2−6.
(52) Nmegbu, C. J.; Ohazuruike, L. Wellbore Instability in Oil Well Drilling: A Review. *Int. J. Eng. Res.* **2014**, *10* (5), 11−20.
(53) Lei, M.; Huang, W.; Sun, J.; Shao, Z.; Wu, T.; Liu, J.; Fan, Y. Synthesis of Carboxymethyl Chitosan as an Eco-Friendly Amphoteric Shale Inhibitor in Water-Based Drilling Fluid and an Assessment of Its Inhibition Mechanism. *Appl. Clay Sci.* **2020**, *193* (April), No. 105637.
(54) Luo, Z.; Wang, L.; Yu, P.; Chen, Z. Experimental Study on the Application of an Ionic Liquid as a Shale Inhibitor and Inhibitive Mechanism. *Appl. Clay Sci.* **2017**, *150* (June), 267−274.
(55) Xu, J.-g.; Qiu, Z.; Zhao, X.; Zhong, H.; Huang, W. Study of 1-Octyl-3-Methylimidazolium Bromide for Inhibiting Shale Hydration and Dispersion. *J. Pet. Sci. Eng.* **2019**, *177*, 208−214.
(56) Xu, J.-g.; Qiu, Z.; Zhao, X.; Zhong, H.; Huang, W. Study of 1-Octyl-3-Methylimidazolium Bromide for Inhibiting Shale Hydration and Dispersion. *J. Pet. Sci. Eng.* **2019**, *177* (Feb), 208−214.
(57) Mohan, K. K.; Fogler, H. S. Effect of pH and Layer Charge on Formation Damage in Porous Media Containing Swelling Clays. *Langmuir* **1997**, *13* (10), 2863−2872.
(58) Murtaza, M.; Kamal, M. S.; Hussain, S. M. S.; Mahmoud, M.; Syed, N. A. Quaternary Ammonium Gemini Surfactants Having Different Spacer Length as Clay Swelling Inhibitors: Mechanism and Performance Evaluation. *J. Mol. Liq.* **2020**, *308*, No. 113054.
(59) He, Z.; Yang, Y.; Qi, J.; Lin, X.; Wang, N.; Wang, L.; Dai, H.; Lu, H. Hyperbranched Polymer Nanocomposite as a Potential Shale Stabilizer in Water-Based Drilling Fluids for Improving Wellbore Stability. *J. Mol. Liq.* **2024**, *395* (Dec), No. 123903.
(60) Tian, Y.; Liu, X.; Luo, P.; Huang, J.; Xiong, J.; Liang, L.; Li, W. Study of a Polyamine Inhibitor Used for Shale Water-Based Drilling Fluid. *ACS Omega* **2021**, *6* (23), 15448−15459.
(61) Ji, L.; Guo, Q.; Friedheim, J.; Zhang, R.; Chenevert, M.; Sharma, M. Laboratory Evaluation and Analysis of Physical Shale Inhibition of an Innovative Water-Based Drilling Fluid with Nanoparticles for Drilling Unconventional Shales. *Soc. Pet. Eng. - SPE Asia Pacific Oil Gas Conf. Exhib. 2012, APOGCE 2012* **2012**, *2*, 1146−1157.

https://doi.org/10.1021/acsomega.4c01632
ACS Omega 2024, 9, 21365−21377